Kinetics of the Sodium Carbonate–Sulfur Dioxide Reaction

The kinetics of the SO_2-Na_2CO_3 reaction were studied at 353 to 413 K and atmospheric pressure with thermal gravimetric analysis data. Since the reaction is very fast, special precautions were taken to operate at conditions such that transport effects did not influence results. The data indicated that Na_2SO_3 was formed by two paths: direct reaction, and adsorption of SO_2 followed by conversion of adsorbed SO_2 to adsorbed CO_2 and finally desorption to final product. Rate constants were evaluated for each step in the proposed mechanism. Product distribution predicted from the rate constants agreed well with the distribution calculated from the experimental data at temperatures from 353 to 413 K. At 413 K the results suggested a change in mechanism.

Shoichi Kimura, J.M. Smith
University of California
Davis, CA 95616

Introduction

Recent research on gas-solid reactions has emphasized the importance of pore structure. Models have been developed to interpret the effect on reaction rate of pore-structure changes during reaction (Bhatia and Perlmutter, 1981a,b; Bhatia, 1985; Ramachandran and Smith, 1977; Ramachandran and Doraiswamy, 1982; Prasannan et al., 1985). They may be classified into three groups: those taking into account the variation of reacting surfaces with time, those analyzing the change in size of pores, and those based on product-layer diffusion. Often the kinetics of the reactions themselves are not well established. The rate equation used is frequently of an overall form, that is, a power-law rate expression.

The reaction of solid carbonates with sulfur dioxide is often employed as an application of the analyses to actual systems (Hartman and Coughlin, 1974; Dogu, 1981; Ramachandran and Smith, 1977; Bhatia and Perlmutter, 1981; Bhatia, 1985; Prasannan et al., 1985). The practical objective is sulfur removal from combustion gases. With Na_2CO_3 the reaction occurs at a relatively low temperature. Marecek et al. (1970) and Hartman (1978) found optimal values at 393 to 423 K. In spite of the low temperature, the rate is greater by one to two orders of magnitude than that of the limestone-SO_2 reaction at temperatures around 1,100 K (Hartman, 1978). Also, sodium carbonate reacts completely, while with some limestones the reaction ceases due to pore closure before most of the solid reacts (Hartman and Coughlin, 1974; Dogu, 1981).

Correspondence concerning this paper should be addressed to J.M. Smith.
Shoichi Kimura is on leave from Osaka University, Toyonaka, Osaka 560, Japan.

Active sodium carbonate is obtained by the decomposition of sodium bicarbonate (Wang Hu et al., 1986; Subramanian et al., 1972). The overall kinetics of the reaction of SO_2 with Na_2CO_3 has also been investigated. However, a first-order rate equation (Dogu, 1986; Marecek et al., 1970) or a Langmuir-Hinshelwood type expression (Erdos, 1969) has been employed for the overall reaction to produce sodium sulfite and CO_2. Although adsorption equilibrium for SO_2 is assumed, the mechanisms of the adsorption step and the effect of temperature and gas composition on the reaction are not well understood (Dogu, 1986; Marecek et al., 1969).

Our objective is to study the intrinsic kinetics and the mechanism of the overall reaction. Using thermal gravimetric analysis (TGA), the rate of adsorption of SO_2 as well as the rates of the following surface reactions and desorption of CO_2 were evaluated. The reaction conditions cover temperatures from 353 to 453 K, including the optimum temperature region, and SO_2 concentrations from 0.24 to 5%.

The results suggest two reaction paths. Thus, Na_2CO_3 reacts with SO_2 directly to form the product Na_2SO_3; this is the predominant process at temperatures above 413 K. Also, irreversible SO_2 adsorption at temperatures of 353 to 413 K indicates that the reaction can occur by formation of two different intermediates having identical molecular weight, followed by desorption of CO_2. This process dominates the formation of Na_2SO_3 at temperatures below 393 K. Not only the rate of SO_2 adsorption but also the direct reaction is affected by the adsorbed SO_2. The Na_2CO_3 molecules active for both adsorbing and reacting SO_2 appear to be those not adjacent to adsorbed SO_2. The rate equation for each reaction step, temperature dependence, and the

effect of SO_2 concentration in the range of 0.24 to 5.0%, were established. The proposed mechanism well represents data obtained at temperatures of 413 K and below. At temperatures above 413 K different kinetics are apparently involved.

Experimental Method

Sample preparation

About 4×10^{-4} kg of powdered sodium bicarbonate (Mallincrodt, 99.7% $NaHCO_3$) was subjected to a force of 9,760 kg in a 1.2×10^{-2} m dia. mold for 60 s. The resultant cylindrical pellets were then crushed and sieved. Particles having an average size in the range of 6.1×10^{-5} to 2.95×10^{-4} m were used for reaction experiments and those in the range of $4.2–5.9 \times 10^{-4}$ m for pore-volume measurements.

Apparatus and Procedures

Thermal decomposition of $NaHCO_3$ and subsequent reaction experiments of Na_2CO_3 with SO_2 were carried out using a Perkin-Elmer TGA (model TGS-2). Figure 1a schematically shows the apparatus. Since the reaction is extremely fast, special care was taken to avoid transport effects. Samples of $NaHCO_3$ particles were placed on a thin layer of fine glass fibers in a platinum basket. The basket was placed in the furnace, hung on platinum wire connected to the microbalance, as shown in Figure 1b. The stream of helium or reactant gas entered through a small tube directly into the furnace beneath the sample basket.

The concentration of SO_2 in the reactant gas was adjusted in the gas reservoir by mixing SO_2 with helium. The thermobalance unit was purged by a small continuous stream of helium of 3.3×10^{-8} m^3/s to prevent contamination by SO_2. This stream can be neglected in volume compared to the main stream.

Since oxygen could react with product sodium sulfite, high-purity (99.995%) helium was used. In advance of each decomposition experiment the whole system was evacuated at room temperature for 15 min to eliminate oxygen. The sample was then heated to the prescribed decomposition temperature (453 K) in the stream of helium at the rate of 5.3 K/s. Simultaneously, the change in sample weight was monitored. Two minutes after the sample weight reached a constant value, the sample was cooled to the desired reaction temperature in the stream of helium. The ultimate weight of the sample agreed with that predicted from the stoichiometry of decomposition of $NaHCO_3$ to Na_2CO_3.

The flow rate of reactant gas was adjusted to the same value as that of helium used for decomposition. The reactant gas was then introduced into the furnace by quickly switching the four-way valve shown in Figure 1a. The change in sample weight was again monitored.

To obtain conversion vs. time data, the reaction was terminated at any time by quickly changing the reactant gas back to helium with the four-way valve. When the sample weight attained a constant value, the sample was heated to 573 K in the helium stream and held at this temperature for 1 min to gasify any adsorbed species. The sample was then cooled to the reaction temperature and the final weight of the sample measured.

Observation of pore structure

Na_2CO_3 and also product Na_2SO_3 particles were occasionally taken from the furnace after cooling to room temperature in the stream of helium and subjected to pore-volume measurement and microscopic examination.

Pore-volume distribution was determined in a mercury porosimeter (American Instrument Co.) that is capable of measuring pore diameters as low as 3 nm at the maximum pressure.

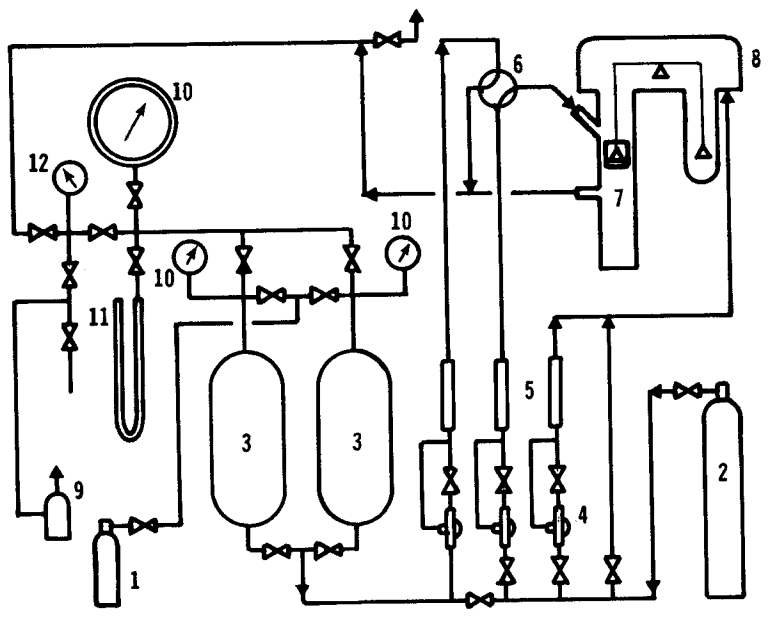

(a) 1, SO_2 Cylinder; 2, Helium Cylinder; 3, Reservoir; 4, Gas Flow Regulator; 5, Flow Meter; 6, 4-Way Valve; 7, Furnace; 8, Microbalance; 9, Vacuum Pump; 10, Pressure Gauge; 11, Manometer; 12, Vacuum Gauge

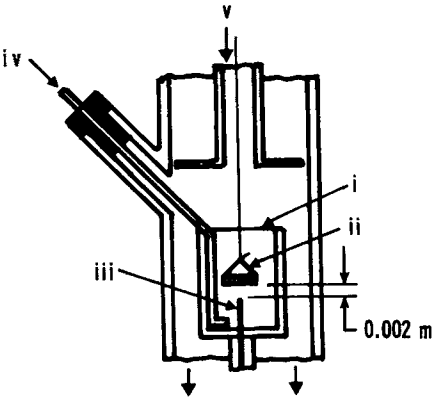

(b) i : Furnace 0.012m i.d. x 0.020m ht.
ii : Sample Basket
iii : Thermocouple
iv : Helium or Reactant Gas
v : Helium

Figure 1. Experimental apparatus.

Microscopic photographs were taken with a scanning electron microscope (International Scientific Instrument, DS130). SEM specimens were prepared by gold-sputter coating procedures.

Results

Properties of solid materials

SEM photographs of the pore structure of Na_2CO_3 and Na_2SO_3 with magnifications of 13,400 and 22,200, respectively, showed the following characteristics. The original $NaHCO_3$ (not shown) is composed of rather large dense grains 10^{-5} to 10^{-4} m in size. After decomposition to Na_2CO_3, these grains become very porous and appear to be composed of an assembly of much smaller grains having an average diameter of about 100 nm. The grainy porous structure is still retained after conversion into Na_2SO_3. Sodium carbonate obtained by decomposition at 473 K has many filaments formed on the grains. This is not observed for Na_2CO_3 obtained at 453 K or below. Reaction experiments showed that the formation of filaments resulted in a slight increase in rate. However, this phenomenon was not studied further. The Na_2CO_3 samples used to study reaction kinetics were always prepared by decomposition at 453 K.

Cumulative pore-volume vs. pore-radius data were measured for Na_2CO_3 obtained by decomposition at 453 K and for Na_2SO_3 obtained by reaction at 393 K. The total pore volume decreases significantly from 4.78×10^{-4} to 3.02×10^{-4} m^3/kg as a result of reaction.

Preliminary experiments

Transport effects were examined by changing sample mass, particle size, and flow rate of reactant gas. Runs were made at 393 K with a gas composition of 1.5% SO_2. Figure 2 indicates the results in terms of the normalized weight change $\overline{W}_t$, defined as the actual weight change (including adsorbed species) divided by the maximum weight change due to reaction only (no adsorption), or

$$\overline{W}_t = \frac{W_t - W_{to}}{W_{to}(r - 1)} \tag{1}$$

The effect of sample mass is indicated by the data obtained with a gas flow rate of 4.17×10^{-6} m^3/s and particles of 8.8×10^{-5} m dia. The decrease in weight change for the larger sample masses is likely due to mass transfer resistance in the multiple layers of particles. Sample size does not significantly affect the weight change curve when the mass is smaller than about 3.3×10^{-7} kg.

The effect of particle size is shown in Figure 2 by the data obtained at a constant gas flow rate of 4.17×10^{-6} m^3/s with sample mass in the range of $1.7–2.6 \times 10^{-7}$ kg. When particles have an average size smaller than 1.14×10^{-4} m, there is no significant difference between the curves. When particle size becomes as large as 1.92×10^{-4} m the weight vs. time curve is no longer identical with the others. These results show that

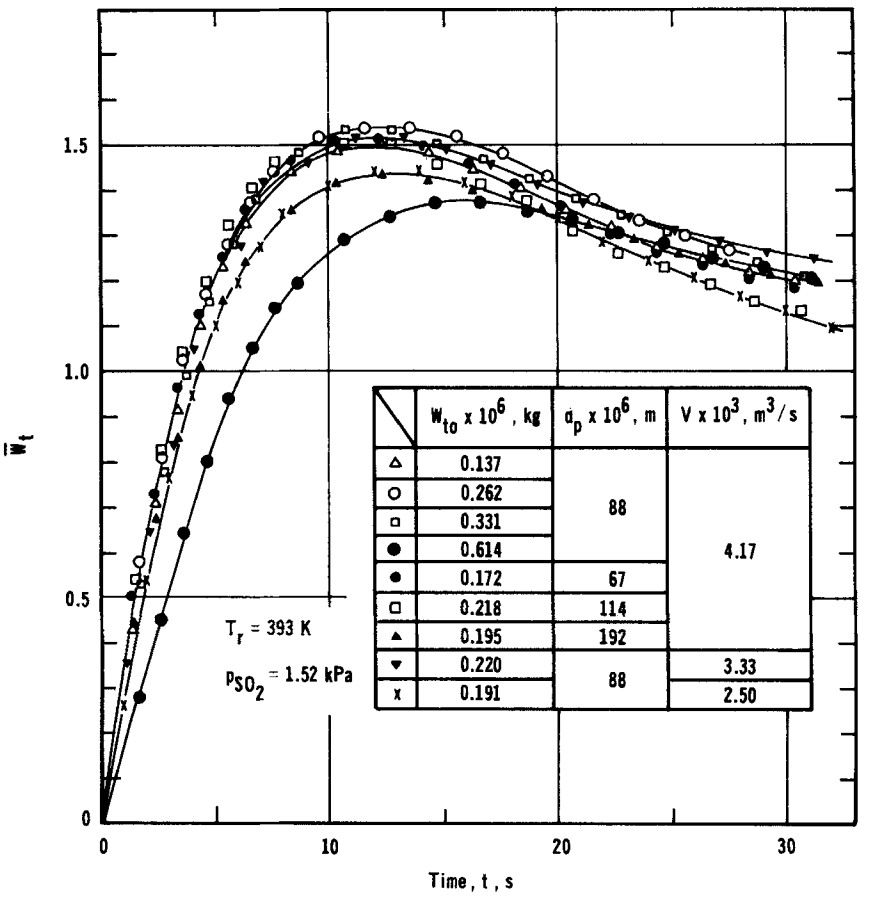

Figure 2. Effect of sample mass, particle size, and flow rate of reactant on sample weight.

intraparticle transport can be neglected for particles smaller than 1.14×10^{-4} m.

The effect of gas flow rate is indicated by the data obtained using sample particles with an average size of 8.8×10^{-5} m and with a sample mass in the range of $1.9–2.6 \times 10^{-7}$ kg. The weight vs. time curves are essentially the same when the flow rate of reactant gas is greater than 3.33×10^{-6} m^3/s.

Subsequent kinetic data were obtained using sample particles of 8.8×10^{-5} m at a flow rate of 4.17×10^{-6} m^3/s and a sample mass of $1.5–2.5 \times 10^{-7}$ kg. The experimental conditions employed in this work are summarized in Table 1. Since high sensitivity of the microbalance was required for the small particles and high gas flow rate, the monitored value of weight was slightly affected by the buoyancy due to gas flow and introduced some uncertainty. Consequently, the reproducibility of data resulted in a maximum error of about 10%. However, much larger errors would have been introduced by the intrusion of transport effects.

Kinetics data for the Na_2CO_3-SO_2 reaction

The overall reaction of Na_2CO_3 (solid, s) with SO_2 (gas, g) is

$$\underset{(A)}{Na_2CO_3(s)} + SO_2(g) \rightarrow \underset{(D)}{Na_2SO_3(s)} + CO_2(g)$$

When Na_2CO_3 is completely converted into Na_2SO_3, the normalized weight change $\overline{W}_t$ of the sample, defined by Eq. 1, should become 1.0. However, as shown in Figure 2, the weight of the sample first exceeds the value it should reach at complete conversion and then goes down toward 1.0 at longer times. This excess weight is attributed to adsorption of SO_2 and CO_2 on the solid; the sample weight is the sum of weights of solid and adsorbates.

Figure 3 displays a series of data at a constant 1.5% SO_2 concentration and at 393 K when the reactions were terminated by switching the reactant gas to helium at 2, 5, 7, 10, 20, and 28.5 s. The total sample weight decreases when pure helium is introduced and finally attains a constant value. The decrease is attributed to desorption of adsorbates. The ultimate sample weight so obtained corresponds to the weight of a mixture of unconverted Na_2CO_3 and product Na_2SO_3 free from adsorbates. When the sample was heated to 573 K, after the weight reached a constant value no further decrease in weight was observed.

Figure 4 shows similar results at a lower temperature, 373 K. The rate of change of sample weight, which corresponds to the desorption rate at the termination of reaction, depends on the length of reaction time and on the reaction temperature. When the gas flow is first changed to helium, at any beginning stage of reaction, the sample weight remains unchanged for a period of time and then gradually decreases. The time period during which the sample weight does not change becomes longer as

Table 1. Experimental Conditions for Kinetics Data

Decomposition temp., T_d = 453 K
Reaction temp., T_r = 353–453 K
Flow rate of reactant gas, $V = 4.17 \times 10^{-6}$ m^3/s*
Partial pressure of SO_2, p_{SO_2} = 0.243–5.07 kPa (0.24–5.0%)
Dia. of sample particles, $d_p = 7.4 \times 10^{-5}$ to 1.04×10^{-4} m
Wt. of sample, $W_{to} = 1.5–2.5 \times 10^{-7}$ kg

*at 298 K and 101.3 kPa

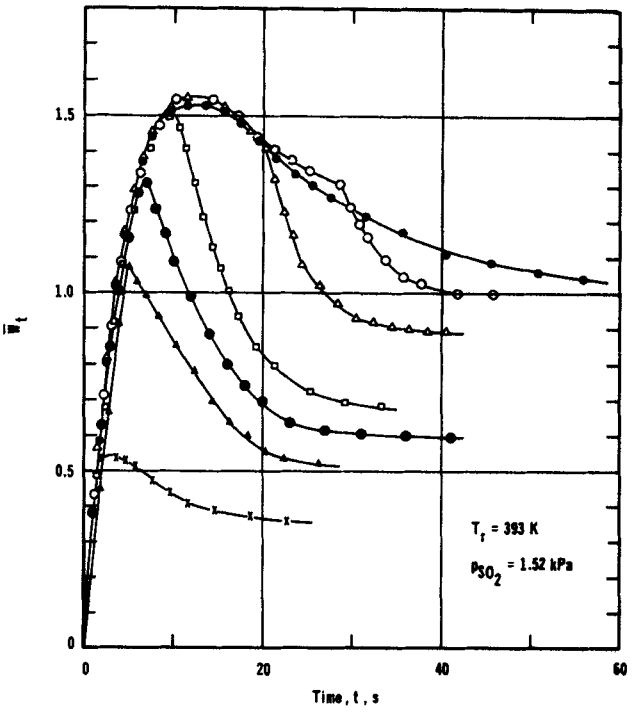

Figure 3. Change in sample weight when reaction is terminated at various times.
T_d = 453 K; T_r = 393 K

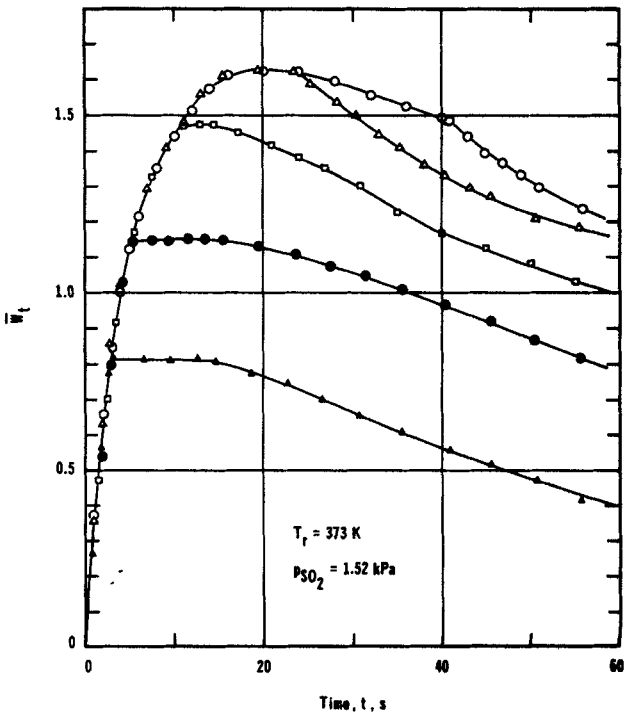

Figure 4. Change in sample weight when reaction is terminated at various times.
T_d = 453 K; T_r = 373 K

reaction times becomes shorter. While the sample weight remains unchanged neither desorption nor a reaction involving weight change occurs. Thus at the lower temperatures where this constant weight period exists, the adsorption of SO_2 is irreversible. When the reaction temperature is high, the period of unchanging weight becomes short and tends to disappear, as shown in Figure 3.

The rate of change in the total sample weight is the sum of the rate of increase due to adsorption and the rate of decrease due to desorption. There is no adsorption when the reaction is terminated, that is, when the gas stream is changed from the SO_2 mixture to helium. Therefore, the rate of decrease in total weight, at the instant when the reaction is terminated, directly corresponds to the rate of desorption at this time. Thus the desorption rate $-(d\overline{W}_t/dt)_d$ can be evaluated by taking the slope of the desorption curve in Figures 3 and 4 at the time when the gas stream is changed to pure helium and the reaction is terminated. The results are shown in Figure 5, where the desorption rate is plotted vs. the time at which the reaction was terminated. The desorption rate is greatest at 393 K and decreases as reaction temperature is either lower or higher. At temperatures below 393 K this rate is zero during the initial stage of reaction. The time of the zero-rate period becomes longer as the temperature decreases. At temperatures of 413 and 453 K the desorption rate has a nonzero value even during the beginning stage of reaction: desorption occurs from the beginning of reaction.

Since SO_2 can be the only adsorbate on the solid during a period just after the reaction is initiated, these data suggest that SO_2 does not desorb once it has been adsorbed. Therefore, the decrease in sample weight during the entire course of reaction is attributed solely to the desorption of CO_2, while the increase in the weight may result from the adsorption of SO_2 and a possible direct exchange of SO_2 with CO_2 without adsorption and desorption steps.

Figure 6 shows the variation with time of sample weights $\overline{W}_t$ and $\overline{W}$ observed at different temperatures and at a constant SO_2 concentration of 1.5%. Note that $\overline{W}$, which is the weight ultimately attained after the reaction was terminated, Eq. 6, is plotted against the corresponding time at which the reactant gas was switched to helium. Thus $\overline{W}_t$ and $\overline{W}$ are for the same time values. Figure 7 is a similar plot showing the effect of SO_2 concentration

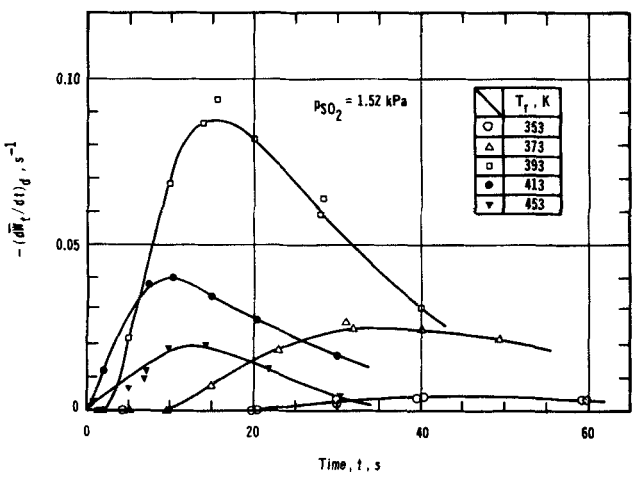

Figure 5. Rate of change in sample weight at the instant when reaction is terminated in helium gas.

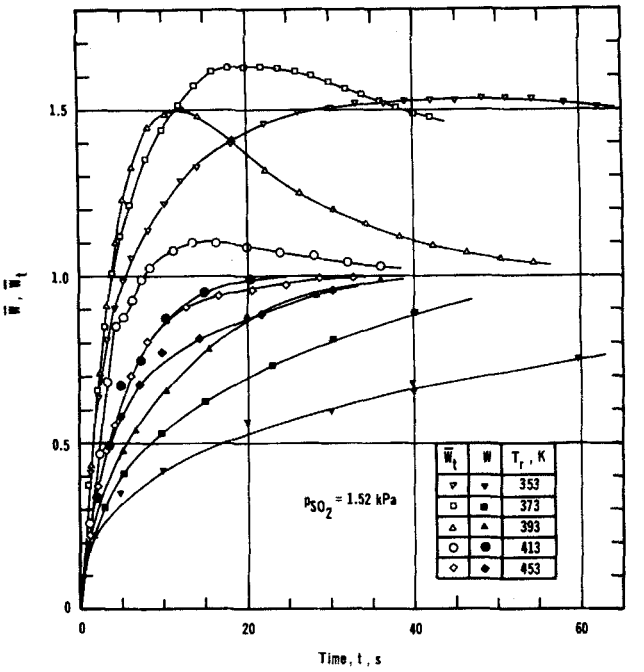

Figure 6. Effect of temperature on sample weights $\overline{W}_t$ and $\overline{W}$.

at 373 K on $\overline{W}_t$ and $\overline{W}$. The difference, $\overline{W}_t - \overline{W}$, between the sample weight at any time t and the weight attained after the reaction was terminated at that time, corresponds to the quantity of adsorbates at that time. The amount of adsorbed molecules is significant at low temperatures but small at high temperatures, as shown later in Figure 8. However, the quantity of adsorbates does not change much with the SO_2 concentration although it takes a longer time for adsorbates to accumulate

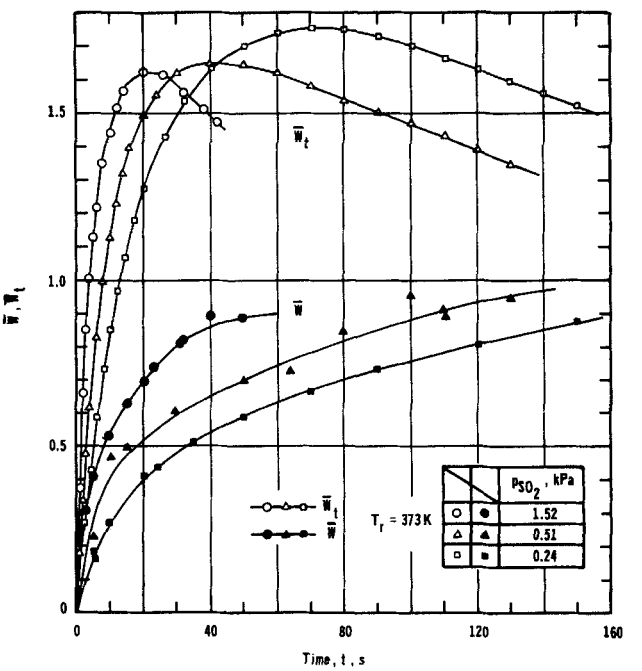

Figure 7. Effect of SO_2 concentration on change in sample weights $\overline{W}_t$ and $\overline{W}$ with time.

when the concentration is low. The total weight $\overline{W}_t$ shows a stepwise change when it reaches about 0.9 at 413 K. This phenomenon was observed at temperatures above 403 K.

Reaction mechanism

In view of the data, we may assume for the Na_2CO_3-SO_2 reaction that:

1. The adsorption step of SO_2 is irreversible.
2. There is at least one reaction step in which some intermediate species of different kinds, but of the same molecular weight, are formed (constant weight period shown in Figures 3 and 4).

Other steps in the mechanism may not be intrinsically irreversible, but concentrations of CO_2 are so low that the reverse reactions are not significant. The weight of sample during the course of reaction is given, in terms of moles of reactant, intermediates, and product at any time, as

$$W_t = M_A N_A + M_B\left(\sum_i N_i\right) + M_D N_D \tag{2}$$

The weight of the sample, W, after the reaction is terminated in the stream of helium and when all the intermediates have been completely converted to product, consists of unreacted Na_2CO_3 and product Na_2SO_3. Part of the Na_2SO_3 has come from the conversion of intermediates during the time, after reaction, that the gas has been switched to pure helium. Hence, W can be expressed in terms of the weight of intermediates at the termination of reaction:

$$W = M_A N_A + M_D\left(\sum_i N_i + N_D\right) \tag{3}$$

Stoichiometry relates the moles of solids to the initial moles N_{Ao} of Na_2CO_3:

$$N_A + \left(\sum_i N_i\right) + N_D = N_{Ao} \tag{4}$$

With Eq. 4 and $W_{to} = M_A N_{Ao}$, Eqs. 2 and 3 may be represented in terms of the normalized weight change as

$$\overline{W}_t = \frac{W_t - M_A N_{Ao}}{N_{Ao}(M_D - M_A)} = 1 - n_A + \left(\frac{M_B - M_D}{M_D - M_A}\right)\sum_i n_i \tag{5}$$

and

$$\overline{W} = \frac{W - M_A N_{Ao}}{N_{Ao}(M_D - M_A)} = 1 - n_A \tag{6}$$

Equations 5 and 6 provide a relation between the molar fraction of intermediates and difference $\overline{W}_t - \overline{W}$; that is,

$$\sum_i n_i = \left(\frac{M_D - M_A}{M_B - M_D}\right)(\overline{W}_t - \overline{W}) \tag{7}$$

Equation 4 may be rewritten as

$$n_A + \left(\sum_i n_i\right) + n_D = 1 \tag{8}$$

With these concepts about the reaction mechanism, n_A, $\Sigma\, n_i$ and n_D can be calculated from the experimental data for $\overline{W}_t$ and $\overline{W}$ using Eqs. 6–8. As indicated by Eq. 6, $\overline{W}$ is equivalent to the fraction of Na_2CO_3 converted into intermediate species and also possibly into the product.

The sum of molar fractions, $\Sigma_i\, n_i$, of intermediates and the molar fraction of product n_D calculated from Eqs. 6–8 are plotted against time in Figures 8 and 9. The accumulation of intermediates is more pronounced at low temperature. This confirms the conclusion from the data in Figure 5 showing that the rate of desorption of CO_2 is low at low temperatures. The formation rate of Na_2SO_3 also is low at low temperature, as shown in Figure 9. Conversely, at higher temperatures the accumulation of the intermediates decreases, resulting in the low desorption rate of CO_2 as shown in Figure 5. However, Figure 9 indicates that the formation of Na_2SO_3 becomes significant in a short time at high temperature. We may assume from this observation that Na_2SO_3 is also formed through a step that does not include the adsorption of SO_2 and the desorption of CO_2.

The cumulative amount of Na_2SO_3 produced through the desorption of CO_2 may be calculated by integrating with respect to time the desorption rate $-(d\overline{W}_t/dt)_d$ shown in Figure 5:

$$n_{D,1} = \left(\frac{M_D - M_A}{M_B - M_D}\right)\int_0^t -\left(\frac{d\overline{W}_t}{dt}_d\, dt\right) \tag{9}$$

Since we know the total amount of Na_2SO_3 produced at any time, the Na_2SO_3 produced without going through the desorption step may also be calculated from the expression

$$n_{D,A} = n_D - n_{D,1} \tag{10}$$

Figure 10 displays the results obtained at different conditions as $n_{D,A}$ plotted against $1 - n_A$, the fraction of Na_2CO_3 converted. The amount of Na_2SO_3 produced through a step other than CO_2 desorption is proportional to the amount $1 - n_A$ of Na_2CO_3 converted. The proportionality coefficient is independent of the SO_2 concentration. At temperatures above 413 K, more than 80% of the Na_2SO_3 (at complete conversion) is formed without going through the CO_2 desorption step. At low temperatures $n_{D,A}$ is small, and the step involving CO_2 desorption is the predominant

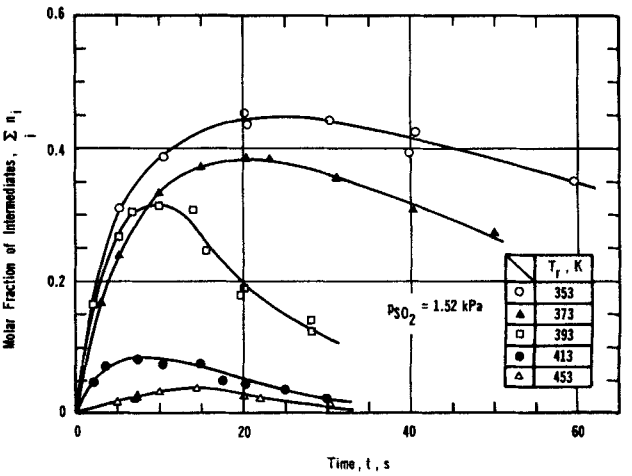

Figure 8. Accumulation of intermediates at various temperatures.

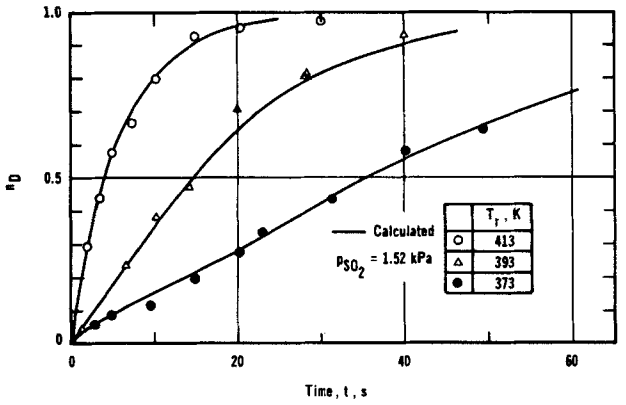

Figure 9. Cumulative amount of product Na_2SO_3.

path to produce Na_2SO_3. Scattering of data at low temperature may be attributed to the small difference between n_D and $n_{D,1}$.

These results suggest a third assumption: Na_2SO_3 can be formed directly from Na_2CO_3 involving neither the adsorption of SO_2 nor the desorption of CO_2.

On the basis of the three assumptions, the reaction mechanism may be written as

$$\underset{(A)}{Na_2CO_3(s)} + SO_2(g) \xrightarrow{k_4} \underset{(D)}{Na_2SO_3(s)} + CO_2(g)$$

$$\underset{(A)}{Na_2CO_3(s)} \xrightarrow{k_1} \underset{(B)}{(Na_2CO_3 \cdot SO_2)}$$

$$\underset{(D)}{Na_2SO_3(s)} \xrightarrow{k_3} CO_2(g)$$

$$\underset{(B)}{(Na_2CO_3 \cdot SO_2)} \xrightarrow{k_2} \underset{(C)}{(Na_2SO_3 \cdot CO_2)}$$

The first two rate constants, k_4 and k_1, represent the direct exchange of SO_2 with CO_2 to form Na_2SO_3, and the chemical adsorption of SO_2 on Na_2CO_3, respectively. The third step is an exchange reaction of SO_2 with CO_2 in the solid phase in which two kinds of intermediates are assumed. The fourth step is the desorption of CO_2 from the intermediate to yield Na_2SO_3.

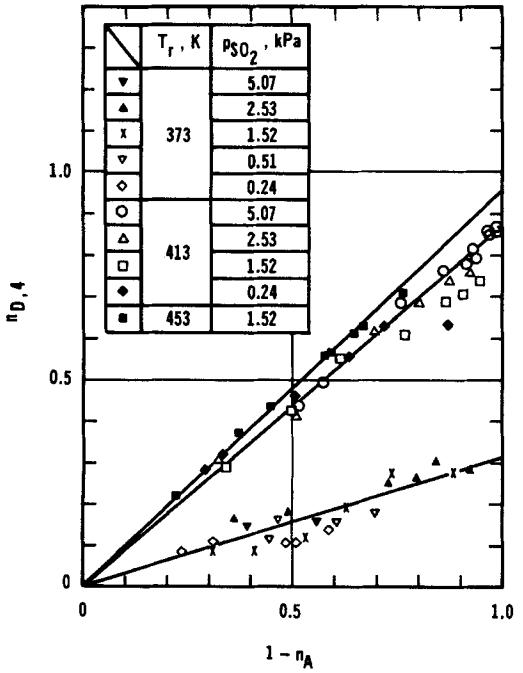

Figure 10. Amount of Na_2SO_3 produced by direct reaction.

Discussion

From the proposed mechanism and the experimental data, rate constants can be calculated. Once the rate constants have been determined, all n values can be predicted for comparison with molar fractions evaluated from the experimental data. The equations and results of these calculations are presented next.

Evaluation of $k_1 + k_4$

The data for the unconverted fraction, n_A, of Na_2CO_3 are plotted on semilogarithmic coordinates in Figure 11. The curves become linear as temperature increases, with the exception of data at 453 K. At 413 K the data suggest that the rate of disappearance of Na_2CO_3 by adsorption (k_1) and direct reaction (k_4) may be approximated by

$$-\frac{dn_A}{dt} = (k_1 + k_4)\, n_A \tag{11}$$

However, at 393 K and increasingly at lower temperatures, the curves deviate from a linear relationship. Figure 8 shows that the lower the reaction temperature, the larger the fraction of intermediates. Thus, the slower rate of conversion at low times in the first two reaction steps is due to the accumulation of $Na_2CO_3 \cdot SO_2$ (B) and/or $Na_2SO_3 \cdot CO_2$ (C). This is demonstrated in Figure 12 where $-(dn_A/dt)/n_A$, obtained from the slope of the $\bar{W}$ vs. t curves (Figures 6 and 7), is plotted against $(n_B + n_C)/n_A$, the moles of intermediates formed per mole of Na_2CO_3. At low temperatures the linear relationships hold in the region where $(n_B + n_C)/n_A$ is not large. For large values of intermediates, $-(dn_A/dt)/n_A$ becomes independent of $(n_B + n_C)/n_A$.

Since the reactions involving intermediates proceed in series, $Na_2CO_3 \cdot SO_2$ (B) first accumulates and then is converted into $Na_2SO_3 \cdot CO_2$ (C). The intermediate is predominantly $Na_2CO_3 \cdot SO_2$ (B) during the initial stage of reaction. Hence, $n_C \to 0$ and the slower rate of conversion in the first two reaction steps is

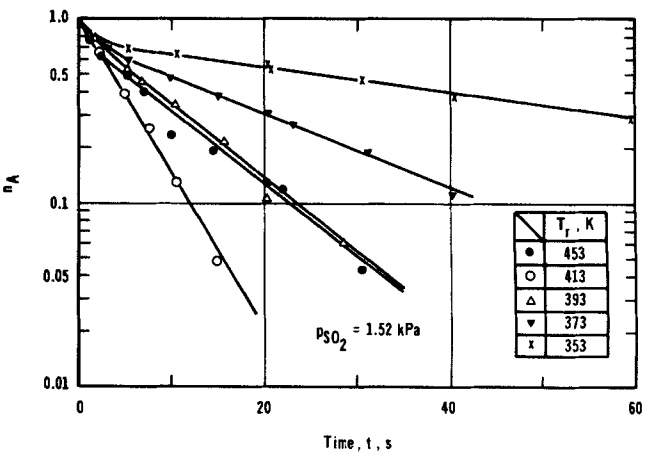

Figure 11. Semilogarithmic plot of unconverted fraction of Na_2CO_3.

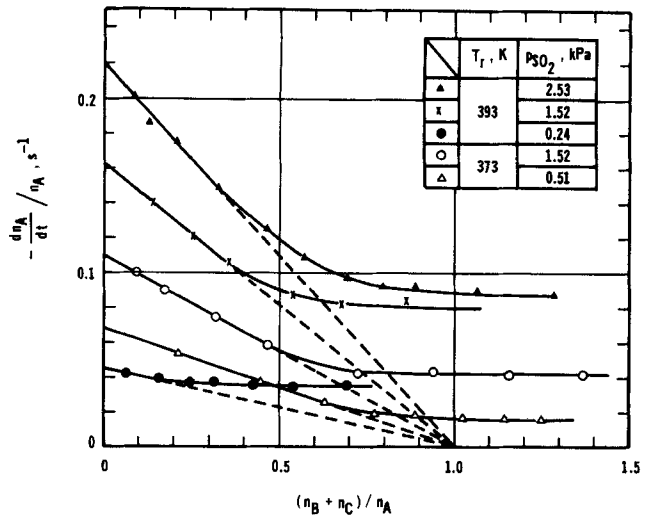

Figure 12. Effect of intermediates on rate of Na_2CO_3 conversion.

attributed to the accumulation of $Na_2CO_3 \cdot SO_2$ alone. The straight lines in Figure 12 correspond to the equation

$$-\left(\frac{dn_A}{dt}\right)\Big/ n_A = a - b\left(\frac{n_B}{n_A}\right)$$

Extrapolation of these lines yields a common intercept on the abscissa at $(n_B + n_C)/n_A \simeq n_B/n_A = 1.0$, showing that $a = b$. When $n_B = 0$, $-(dn_A/dt)/n_A = a$, or $(k_1 + k_4)$, according to Eq. 11. Hence, the effect of intermediates on the rate of conversion of Na_2CO_3 is given by

$$-\left(\frac{dn_A}{dt}\right) = (k_1 + k_4)(n_A - n_B) \qquad (12)$$

Equation 12 suggests that only molecules of Na_2CO_3 which are not the nearest neighbor to $Na_2CO_3 \cdot SO_2$ are active for both the reaction and adsorption steps. Nearest-neighbor reactions may be improbable because of interaction of bonding orbitals, or a repulsive character of adsorbed molecules (Tompkins, 1978).

The intercepts of the straight lines in Figure 12 with the ordinate give values of $(k_4 + k_1)$. Also, Eq. 12 can be used to predict n_B. The sum $(k_1 + k_4)$ is known as well as n_A. Since $n_A = 1 - \overline{W}$, differentiation of the experimental $\overline{W}$ vs. t curves (Figures 6 and 7) gives (dn_A/dt). With known Σn_i, values of n_C can be obtained. Thus n_A, n_B, n_C, and n_D can be calculated at any time using $\overline{W}_t$ and $\overline{W}$ vs. time data and Eqs. 6–8 and 12. For example, Figure 13 shows the variation with time of the molar fraction of each component estimated from the data at 373 K with 1.5% SO_2. Results such as those given in Figure 13 may be used to evaluate k_2 and k_3, separate $k_1 + k_4$, and establish rate equations for the other reaction steps in the temperature range 353 to 413 K.

Evaluation of k_3

Figure 14 shows the rate of CO_2 desorption plotted against the molar fraction n_C of $Na_2SO_3 \cdot CO_2$; the linear relationships suggest a first-order rate equation for the desorption step. With this result, and taking Eq. 12 into account, the formation rate of

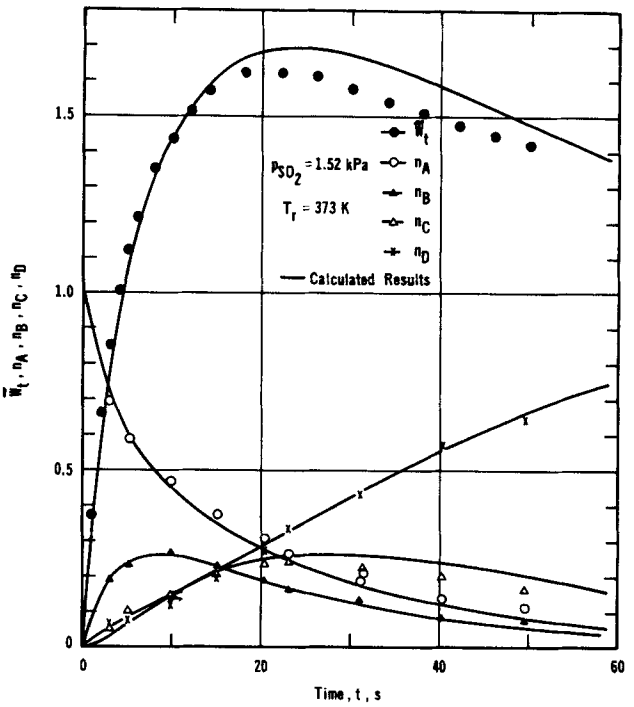

Figure 13. Variation with time of molar fraction of each component.

Na_2SO_3 by direct reaction and by desorption of $Na_2SO_3 \cdot CO_2$ may be written as

$$\frac{dn_D}{dt} = k_4(n_A - n_B) + k_3 n_C \qquad (13)$$

The rate constant k_3 can be evaluated from the slopes of the straight lines in Figure 14. Thus, taking the derivative of Eq. 9

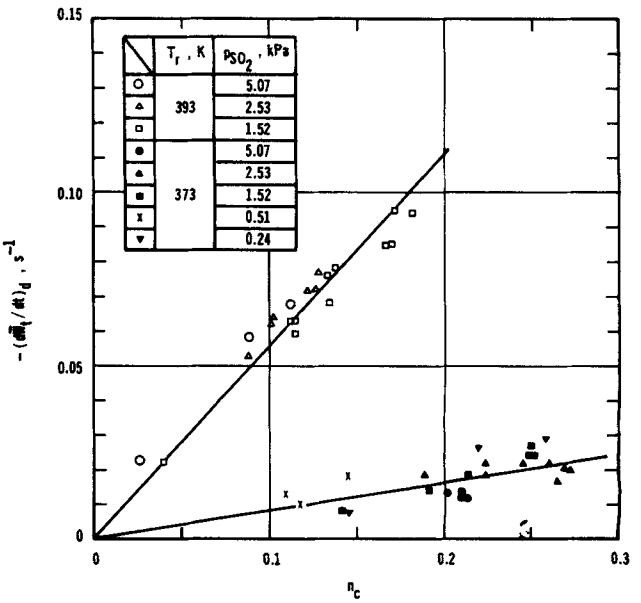

Figure 14. Desorption rate of CO_2 vs. molar fraction of $Na_2SO_3 \cdot CO_2$.

with respect to time gives

$$-\left(\frac{d\bar{W}_t}{dt}\right)_d = \frac{M_B - M_D}{M_D M_A}\frac{dn_{D,1}}{dt} = \frac{M_B - M_D}{M_D M_A} k_3 n_C \qquad (14)$$

Figure 14 indicates that the rate constant k_3 is independent of SO_2 concentration.

Evaluation of k_2 and separation of $k_1 + k_4$

Assuming a first-order rate equation for the conversion of $Na_2CO_3 \cdot SO_2$ to $Na_2SO_3 \cdot CO_2$, we have for the accumulation of $Na_2SO_3 \cdot CO_2$

$$\frac{dn_C}{dt} = k_2 n_B - k_3 n_C \qquad (15)$$

Combining Eq. 15 with Eq. 13 gives

$$\frac{d}{dt}(n_C + n_D) = k_4 (n_A - n_B) + k_2 n_B \qquad (16)$$

Integration of Eq. 16 and some algebraic manipulation using Eq. 12 yields

$$\frac{n_C + n_D}{1 - n_A} = \frac{k_4}{k_4 + k_1} + (k_2)\frac{\int_0^t n_B\, dt}{1 - n_A} \qquad (17)$$

In Figure 15 for 393 K and 1.5% SO_2 the term $(n_C + n_D)/(1 - n_A)$ is plotted against the second term of the righthand side of Eq. 17. The linear relationships lend validity to the first-order assumption for the conversion of $Na_2CO_3 \cdot SO_2$ to $Na_2SO_3 \cdot CO_2$. Also, the group of parallel lines indicates that the rate constant k_2, obtained from the slope of each line, is independent of SO_2 concentration. The intercepts with the ordinate in Figure 15 give $k_4/(k_1 + k_4)$. Since $(k_1 + k_4)$ is known from Figure 12, individual values of k_4 and k_1 can be obtained.

Prediction of molar fractions

Equations 12, 13, and 15 with Eq. 8 give rate equations for the molar fractions of each component in terms of the rate constants. Since all the rate constants are known, these equations may be integrated analytically to predict the variation with time of each molar fraction. The solutions, with initial conditions $n_A = 1, n_B = n_C = n_D = 0$ are

$$n_A = \frac{1}{\alpha - \beta}[(\alpha + k_1 + k_2)e^{\alpha t} - (\beta + k_1 + k_2)e^{\beta t}] \qquad (18)$$

$$n_B = \frac{1}{\alpha - \beta}(e^{\alpha t} - e^{\beta t}) \qquad (19)$$

$$n_C = \frac{k_1 k_2}{(\alpha - \beta)(\alpha + k_3)}e^{\alpha t} + \frac{k_1 k_2}{(\beta - \alpha)(\beta + k_3)}e^{\beta t} + \frac{k_1 k_2}{(\alpha + k_3)(\beta + k_3)}e^{-k_3 t} \qquad (20)$$

$$n_D = 1 - n_A - n_B - n_C \qquad (21)$$

where

$$\alpha, \beta = \frac{-1}{2}[(2k_1 + k_2 + k_4) \pm \sqrt{(2k_1 + k_2 + k_4)^2 - 4k_2(k_1 + k_4)}] \qquad (22)$$

The calculated and experimental results are illustrated in Figure 13 for 373 K for all species, and in Figure 9 for n_D for three temperatures. The rate constants evaluated at individual reaction conditions were used in the calculations. The values of rate constants at 413 K were estimated by extrapolating values at lower temperatures. This was necessary since there is little $Na_2CO_3 \cdot SO_2$ formed at 413 K, and the rate constants could not be evaluated from a plot such as Figure 15.

Effect of SO_2 concentration and temperature

Rate equations have been derived in terms of solid phase composition. Since SO_2 participates in the reaction, the rate constants also should be related to the gas phase composition. It has been shown that the constants k_2 and k_3 are independent of the SO_2 concentration, as expected. Erdos (1969) has assumed a Langmuir-Hinshelwood type rate equation to represent the de-

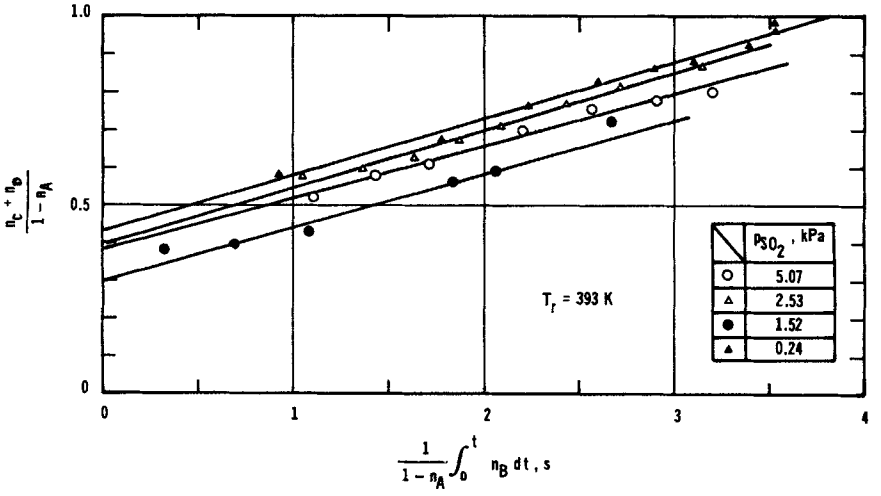

Figure 15. Plot for calculation of k_2, Eq. 17.

pendency of the overall reaction rate on SO_2. Figure 16 for our data confirms this result. The linear relationships suggest that both k_1 and k_4 may be represented by equations of the form:

$$k_i = \frac{k_i' p_{SO_2}}{1 + K_i p_{SO_2}}, \quad i = 1 \text{ or } 4 \tag{23}$$

In the separation of $k_1 + k_4$, using data at a given temperature, the average of values of $k_4/(k_1 + k_4)$ at different SO_2 concentrations was used. This average was evaluated from the intercepts with the ordinate of the linear relationships shown in Figure 15. The average $k_4/(k_1 + k_4)$ for each temperature agreed well with the slope of the corresponding line in Figure 10. These slopes are independent of the SO_2 concentration. Thus, using Eqs. 12 and 13, Eq. 10 is rewritten as

$$n_{D,4} = \frac{k_4}{k_1 + k_4}(1 - n_A) \tag{24}$$

The temperature dependency of k_4' is much greater than that of k_1', Figure 17. The apparent activation energy of k_1' is roughly zero, while that of k_4' is 56.3 kJ/mol. The low value for k_1' suggests that the first chemisorption is nonactivated. It is also implied from the relatively high value of the apparent activation energy for k_4' that the direct reaction of SO_2 with Na_2CO_3 includes an activated step. Since the SO_2 concentration is relatively high, the frequency of SO_2 collisions on Na_2CO_3 is large and of the order of 10^5 times per second (Tompkins, 1978). Thus, one may imagine that very fast physical adsorption and desorption steps for SO_2 precede the chemisorption and reaction of SO_2, and that these preliminary physical steps are in equilibrium in the time scale of reaction. The coverage of solid with condensed SO_2 is considered to be very small so that physical adsorption does not affect the weight of sample. The representation of k_4 and k_1 by Langmuir-Hinshelwood equations may be a

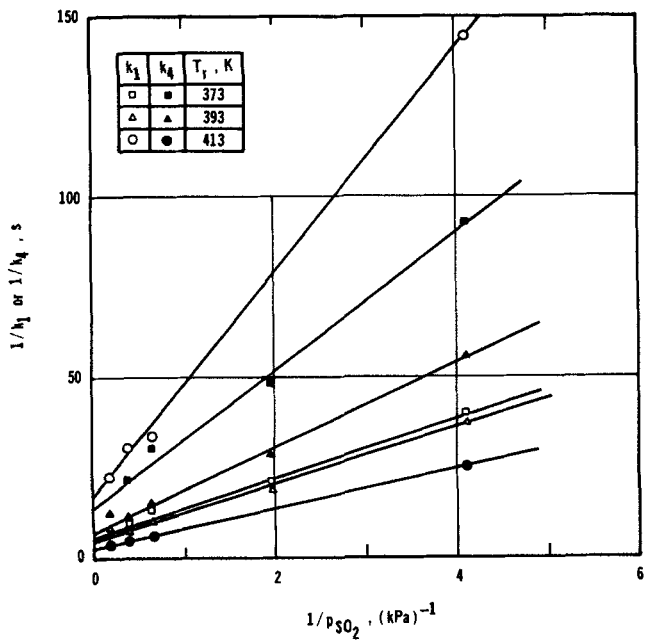

Figure 16. Langmuir-Hinshelwood plot for rate constants k_1 and k_4.

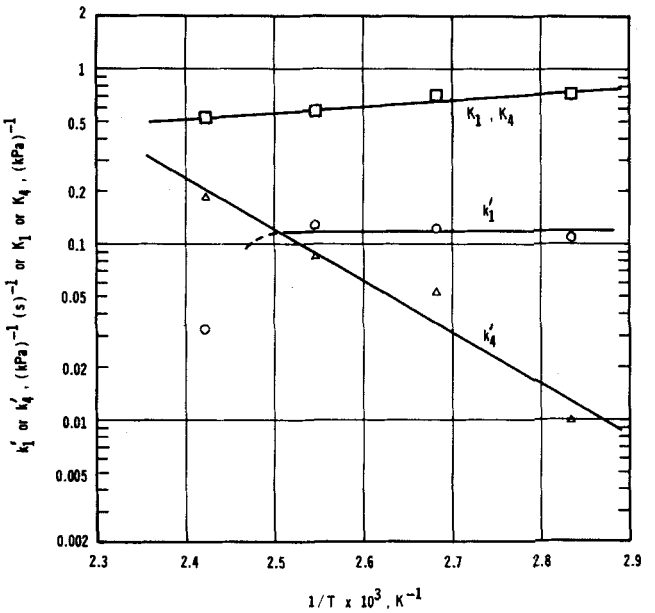

Figure 17. Temperature dependency of kinetics parameters for k_1 and k_4.

result of the physical adsorption equilibrium step preceding the chemical reaction steps. This is consistent with the small value of 6.9 kJ/mol for the heat of adsorption, which is common for K_1 and K_4. The decrease in k_1' at temperatures above 413 K may suggest a change in reaction mechanism. This is shown by the data in Figure 6 indicating that $\overline{W}_t$ has a stepwise change at around $\overline{W}_t \simeq 0.85$ at temperatures above 413 K, as discussed before.

Figure 18 illustrates the temperature dependency of the other two rate constants, k_2 and k_3. The apparent activation energies for k_2 and k_3 are 39.6 and 90.1 kJ/mol, respectively.

Accumulation rate of Na_2SO_3

The accumulation with time of product Na_2SO_3, measured at a fixed SO_2 concentration of 0.3% using a fixed-bed reactor, is given by Hartman (1978). It is stated that the accumulation rate of Na_2SO_3 is independent of temperature in the range 393–

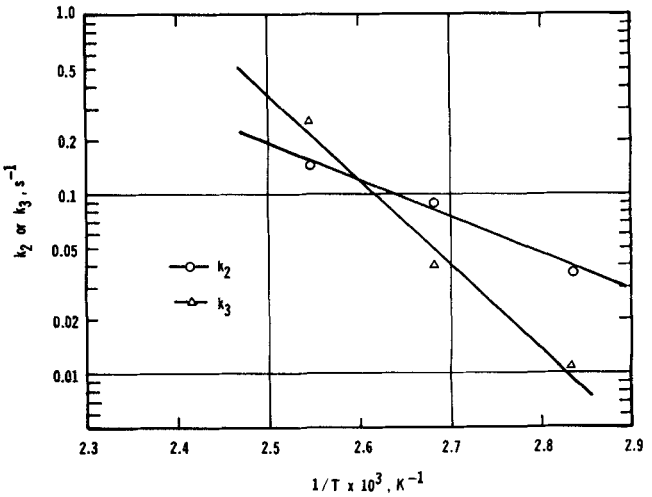

Figure 18. Temperature dependence of k_2 and k_3.

423 K and varies with accumulation of Na_2SO_3. The rate of Na_2SO_3 formation was found to have a maximum value of 0.025 (mol Na_2SO_3/mol Na_2CO_3)(s) when the fraction of Na_2SO_3 is about 0.3. The data of our work at any temperature indicate, as shown in Figure 13, that n_C becomes a maximum when n_D is around 0.2–0.4. The rate of Na_2SO_3 formation is then calculated as 0.011 and 0.019 (mol Na_2SO_3/mol Na_2CO_3)(s) for 393 and 413 K, at 0.24% SO_2, respectively. Both of these values are in good agreement with the results of Hartman.

Acknowledgment

We thank Timur Dogu and Gulsen Dogu, Middle East Technical University, for helpful discussions arranged with the aid of NATO Grant No. RG 83/0892.

Notation

d_p = diameter of solid particles, m
$\bar{d}_p$ = average diameter of particles, m
E = apparent activation energy, kJ/mol
K_1, K_4 = adsorption equilibrium constants, Eq. 23, 1/kPa
k_1, k_2, k_3, k_4 = rate constants for individual steps in proposed mechanism, s^{-1}
k'_1, k'_4 = rate constants, Eq. 23, $kPa^{-1} \cdot s^{-1}$
M = molecular weight, kg/mol
N = number of moles
N_{Ao} = initial moles of Na_2CO_3
N_i = number of moles of intermediate component i
$n_{D,1}$ = molar fraction of Na_2SO_3 produced via desorption of $Na_2SO_3 \cdot CO_2$
$n_{D,4}$ = molar fraction of Na_2SO_3 produced by direct reaction
n_i = molar fraction N_i/N_{Ao} of intermediate i
p_{SO_2} = partial pressure of SO_2, kPa
R_g = gas constant, $kPa \cdot m^3/K \cdot mol$
r = molecular weight ratio of Na_2SO_3 to Na_2CO_3
T_d = decomposition temperature, K
T_r = reaction temperature, K
t = reaction time, s
V = flow rate of reactant gas, m^3/s
W = weight of sample ultimately attained after SO_2 switched to helium and all adsorbates desorbed, kg
$\overline{W}$ = normalized weight of sample, Eq. 6
W_t = total weight of sample, kg
W_{to} = initial weight of sample, kg
$\overline{W}_t$ = normalized total weight of sample, Eq. 5

Subscripts

A = Na_2CO_3
B = $Na_2CO_3 \cdot SO_2$
C = $Na_2SO_3 \cdot CO_2$
D = Na_2SO_3
d = desorption
i = intermediates, $Na_2CO_3 \cdot SO_2$ and $Na_2SO_3 \cdot CO_2$
r = reaction

Literature cited

Bhatia, S. K., "Analysis of Distributed Pore Closure in Gas-Solid Reactions," *AIChE J.*, **31**, 642 (1985).

Bhatia, S. K., and D. D. Perlmutter, "The Effect of Pore Structure on Fluid-Solid Reactions: Application to the SO_2-Lime Reaction," *AIChE J.*, **27**, 226 (1981a).

———, "A Random-Pore Model for Fluid-Solid Reactions. II: Diffusion and Transport Effects," *AIChE J.*, **27**, 247 (1981b).

Dogu, T., "The Importance of Pore Structure and Diffusion in the Kinetics of Gas-Solid Noncatalytic Reactions: Reaction of Calcined Limestone with SO_2," *Chem. Eng. J.*, **21**, 213 (1981).

Dogu, Timur, Aliye Keskin, Gülsen Dogu, and J. M. Smith, "Single-Pellet, Moment Method for Analysis of Gas-Solid Reactions," *AIChE J.*, **32**, 743 (1986).

Erdos, E., "Kinetics of the Reaction between the Solid Sodium Carbonate and the Gaseous Sulfur Dioxide. II: Interpretation of the Excess Kinetic Function by Means of a Microscopic Model," *Coll. Czech. Chem. Commun.*, **34**, 919 (1969).

Hartman, M., "Comparison of Various Carbonates as Absorbents of Sulfur Dioxide from Combustion Gases," *Int. Chem. Eng.*, **18**, 712 (1978).

Hartman, M., and D. W. Coughlin, "Reaction of Sulfur Dioxide with Limestone and the Influence of Pore Structure," *Ind. Eng. Chem. Process Des. Dev.*, **13**, 248 (1974).

Marecek, J., K. Mocek, and E. Erdos, "Kinetics of the Reaction between the Solid Sodium Carbonate and the Gaseous Sulfur Dioxide. IV: Effect of the Gas Phase Composition and of Temperature in an Integral Fixed-Bed Reactor," *Coll. Czecho. Chem. Commun.*, **35**, 154 (1970).

Prasannan, P. C., P. A. Ramachandran, and L. K. Doraiswamy, "A Model for Gas-Solid Reactions with Structural Changes in the Presence of Inert Solids," *Chem. Eng. Sci.*, **40**, 1251 (1985).

Ramachandran, P. A., and L. K. Doraiswamy, "Modeling of Noncatalytic Gas-Solid Reactions," *AIChE J.*, **28**, 881 (1982).

Ramachandran, P. A., and J. M. Smith, "A Single-Pore Model for Gas-Solid Noncatalytic Reactions," *AIChE J.*, **23**, 353 (1977).

Subramanian, K. S., T. P. Radhakrishnan, and A. K. Sundaram, "Thermal Decomposition Kinetics of Sodium Bicarbonate by Differential Thermal Analysis," *J. Therm. Anal.*, **4**, 89 (1972).

Tompkins, F. C., *Chemisorption of Gases on Metals*, Academic Press, New York, Ch. 4, p. 26, Ch. 6, p. 98 (1978).

Wang Hu, J. M. Smith, T. Dogu, and G. Dogu, "Kinetics of Sodium Bicarbonate Decomposition," *AIChE J.*, **32**, 1483 (Sept., 1986).

Manuscript received Aug. 6, 1986, and revision received Dec. 12, 1986.